Available online at www.sciencedirect.com
ScienceDirect
Journal of Catalysis 251 (2007) 59–68
JOURNAL OF CATALYSIS
www.elsevier.com/locate/jcat

Dehydrogenation of *n*-butane over vanadia catalysts supported on θ-alumina

S. David Jackson *, Sreekala Rugmini

WestCHEM, Department of Chemistry, University of Glasgow, Glasgow, G12 8QQ, Scotland, UK

Received 27 March 2007; revised 10 July 2007; accepted 13 July 2007

Available online 23 August 2007

Abstract

Dehydrogenation of *n*-butane was studied over three θ-alumina supported catalysts with different loadings of VO_x. The catalysts were characterised by UV–visible spectroscopy in the as-prepared state and the reduced state. The catalyst with a 1% V loading exhibited a 4+ oxidation state after reduction, whereas the catalysts with 3.5 and 8% V loadings were reduced to a 3+ oxidation state. Oxygen chemisorption gave oxidation state values of 3.8 for the 1% catalyst and 2.6 for the 3.5% catalyst. Both the rate and turnover frequency data confirmed that the sample with the highest proportion of polyvanadate species (3.5V) was the most effective dehydrogenation catalyst. Analysis of the deactivation indicated that butane isomerisation was slow, and deactivation of the isomerisation site was faster than that of the dehydrogenation site. The primary product of butane dehydrogenation was 1-butene, which then isomerised to trans-2-butene. More than three-quarters of the deactivation was due to strongly bound reaction intermediates, which can be removed from the surface at room temperature by treatment in 2% O_2/Ar. The amount of carbon found on each catalyst after removal of the reaction intermediates was alumina < 1V < 3.5V < 8V. Therefore, the VO_x species plays a role in generation of the non-C4 carbonaceous deposits, suggesting either that spillover occurs from the VO_x to the support or that some VO_x sites catalyse the production of coke but do not catalyse dehydrogenation.

Keywords: Dehydrogenation; Butane; Vanadia; Carbon deposition

1. Introduction

Catalytic dehydrogenation of light alkanes is a highly important route for the production of olefins, which are the building blocks of synthetic rubbers, plastics, automotive fuel components, and other valuable chemical products. Industrial chemical processes use chromia- or platinum-based catalysts generally supported on alumina and promoted with alkali metals [1–3]. These processes operate in a cyclical fashion to mitigate against the severe catalyst deactivation that is observed. The high temperatures required to achieve sensible yields for the dehydrogenation reaction lead to catalyst deactivation by coke deposition [4,5]. Numerous studies on the improvement of existing catalysts and the development of vanadia-based dehydrogenation catalysts have been reported [6–10]. Alumina-supported vanadia has been extensively studied over the last few years, with the activity and selectivity of vanadia-supported catalysts modified by the structural and physicochemical properties of the dispersed species supported on the surface [11–15]. It is generally accepted that supported vanadium oxide can exist as isolated monomeric vanadia species, one- or two-dimensional polyvanadate domains, or bulk V_2O_5 crystallites. At low vanadium coverage on the support, isolated monovanadates are the predominant surface species; these condense into polyvanadates and ultimately into bulk V_2O_5 crystallites as VO_x loading increases.

It is notable that the structure of dispersed vanadia changes on exposure to water vapour [16–18]. The extent of this effect depends on the nature of the support and has been studied in detail using XANES, Raman, and UV–visible spectroscopic studies [16]. Silica-supported vanadia is highly susceptible to structural changes on exposure to water at room temperature. Water has little effect on VO_x/Al_2O_3 and VO_x/TiO_2 structure at room temperature, but at high temperature its effect on the surface structure becomes significant [17]. Further, the redox properties of the vanadia catalysts are important for reactions, and the average oxidation state during catalytic operation depends on the relative rates of reduction and reoxidation, as has been discussed previously [12,19–21].

* Corresponding author.
E-mail address: sdj@chem.gla.ac.uk (S.D. Jackson).

0021-9517/$ – see front matter
doi:10.1016/j.jcat.2007.07.015

A series of vanadia catalysts have been prepared and characterised using UV–visible excited Raman spectroscopy [22]. Earlier studies on 1 and 3.5% V on alumina showed that isolated VO_x species are much more effective than polyvanadate species at catalysing carbon deposition during butane dehydrogenation. It also has been observed that polyvanadate species are more effective than isolated vanadia species in dehydrogenation [23]. Here we report the results of our investigation on θ-alumina-supported vanadia catalysts for the direct dehydrogenation of *n*-butane to butenes and butadiene. Three different vanadia loadings (1, 3.5, and 8% V) on θ-alumina were prepared and characterised using X-ray diffraction (XRD), temperature-programmed reduction (TPR), oxygen uptake measurements, and thermal analyses. All three catalysts were evaluated, and temperature-programmed oxidation (TPO) was carried out on the coked catalysts to study the nature of the carbon deposit.

2. Experimental

2.1. Catalyst preparation

The catalysts were prepared by incipient wetness impregnation with θ-alumina as the support. Before impregnation, the alumina was predried at 353 K overnight. An aqueous NH_4VO_3 (>99%, Aldrich) solution was used to prepare the catalyst with a 1% w/w V loading. Oxalic acid (99%, Aldrich) was added into the solutions (NH_4VO_3/oxalic acid = 0.5 molar) for high VO_x loadings (3.5 and 8% V), to ensure dissolution of NH_4VO_3. The θ-alumina support (1/20″ trilobes, surface area = 101 $m^2\,g^{-1}$, pore volume = 0.60 $ml\,g^{-1}$) was supplied by Johnson Matthey, UK. After impregnation, the samples were mixed thoroughly using a rotavap for 2 h at 350 K, dried by purging with air at 393 K overnight, and finally calcined at 823 K for 6 h. The alumina-supported vanadia catalysts with vanadium contents of 1, 3.5, and 8% are designated 1, 3.5, and 8V, respectively.

2.2. XRD analysis

The crystalline structure of the support and catalysts was studied by XRD analysis with a Siemens D 5000 instrument using Cu$K\alpha$ radiation and operated at 40 kV and 30 mA.

2.3. UV–visible diffuse reflectance spectroscopy

UV–visible spectra were obtained using a Varian Cary 5000 Win UV–vis–NIR spectrophotometer equipped with a diffuse reflectance attachment (Harrick) with full environmental control. Catalyst reduction was carried in situ using H_2 at a flow rate of 10 $cm^3\,min^{-1}$.

2.4. Nitrogen adsorption

The surface area of the support and the catalysts were determined from the nitrogen adsorption curve using a Micromeritics Gemini III 2375 surface area analyzer after the samples were degassed at 393 K overnight.

2.5. Thermogravimetric analysis

Thermogravimetric analysis (TGA) of the catalyst precursor and the catalysts was performed using an SDT Q 600 thermal analyser coupled to an online mass spectrometer to analyse evolved gases. Temperature-programmed reduction (TPR) was carried out using the thermal analyser. All measurements were performed with a heating rate of 5 deg min^{-1}.

2.6. Oxygen uptake measurements

Oxygen uptake measurements were carried out at room temperature and also at 873 K after the catalyst was reduced at 873 K using pure H_2. After reduction, the catalyst surface was purged with He for 30 min, and then pulses of oxygen (∼15 μmol) were introduced at the desired temperature until saturation. The amount of oxygen consumed was monitored using an online thermal conductivity detector connected to the effluent of the reactor. The percent uptake is expressed as [O(ads)/M(catalyst)] ×100, assuming an O:M stoichiometry of 1.

2.7. Dehydrogenation activity evaluation

The activity and selectivity of each catalyst were determined using a fixed-bed, continuous-flow reactor. The catalyst (0.25 cm^3) was reduced in pure hydrogen (40 $cm^3\,min^{-1}$) for 1 h at 873 K. The flow was switched to argon, and the system was purged for 30 min. Subsequently, *n*-butane was introduced at a flow rate of 60 $cm^3\,min^{-1}$ at 873 K (GHSV = 14,400) and atmospheric pressure. Reaction products were analysed at regular intervals using an online gas chromatograph (Agilent 6890 Series-FID, Varian Chrompack capillary column CP7568). Regeneration of the catalysts was carried out using 2% O_2/Ar. After a dehydrogenation reaction, the catalyst was purged with argon at 873 K for 0.5 h to remove adsorbed reactant/products from the catalyst surface. The catalyst was then cooled to room temperature in a flow of argon, after which the gas flow was switched to 2% O_2/Ar and the catalyst was heated to 873 K at a programmed heating rate of 10 deg min^{-1}. The temperature was maintained at 873 K until regeneration was complete. The total process was monitored by online mass spectrometry.

The conversion and selectivity were calculated (on a carbon basis) from the reaction products (P), the total amount of *n*-butane fed to the reactor (X), and the amount of butane out (Y) along with the reaction products:

$$\%\text{conversion} = \left[(X - Y)/X\right] \times 100,$$

$$\%\text{selectivity} = \left[P/(X - Y)\right] \times 100.$$

The yield of a specific product was obtained by multiplying the *n*-butane conversion by the corresponding selectivity.

2.8. Microanalysis (C and H) of the spent catalysts

An Exeter Analytica CE-440 elemental analyzer was used to determine %C and %H in the catalysts after evaluation of dehydrogenation activity.

3. Results and discussion

The main characteristics of the vanadia catalysts used in the present study are given in Table 1. A decrease in BET surface area with higher metal loadings was generally observed and could be related to the blockage of pores by the VO_x species. Earlier studies on these catalysts revealed [22,23] that isolated VO_x species dominated at surface densities below 1 V/nm^2, polyvanadates coexisted with monovanadates at surface densities of 1.2–4.4 V/nm^2, and V_2O_5 formed at a surface density >4.4 V/nm^2. The vanadia densities of the catalysts were 1.1 V/mn^2 for the 1V sample, 3.7 V/nm^2 for the 3.5V sample, and 10.4 V/mn^2 for the 8V sample. XRD patterns of the support and the catalysts are shown in Fig. 1. For lower metal loadings, XRD peak position and intensity were the same as for the support alumina, indicating (as expected) that the vanadium oxide species was well dispersed on the surface of the support. However, the XRD pattern for 8V exhibited additional characteristic peaks of crystalline V_2O_5 at 2θ values of 26.3° and 34.6° [12,24].

Table 1
Physicochemical characteristics of the catalysts

Sample	Sample description	Oxygen uptake		Surface area (m^2/g)
		At 300 K	At 873 K	
θ-Alumina	θ-Alumina	–	–	105
1V	1% V on θ-alumina	11.0	60.0	103.5
3.5V	3.5% V on θ-alumina	11.0	122.0	93.6
8V	8% V on θ-alumina	10.2	118.0	76.6

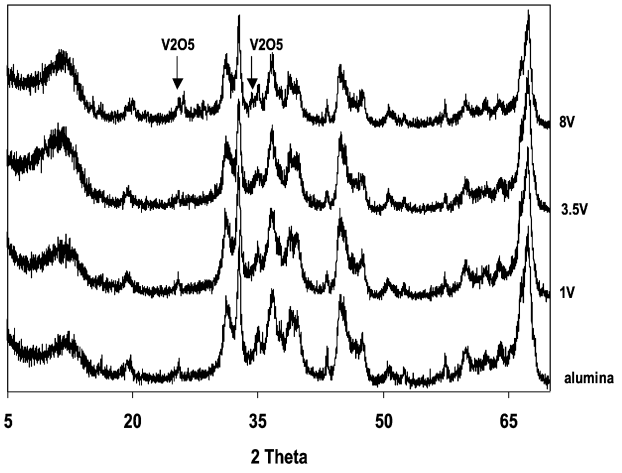

Fig. 1. XRD patterns of θ-alumina and the catalysts.

Each sample was analysed by TGA-H_2. A slow continuous loss of water at the beginning was followed by the reduction of vanadia species. Fig. 2 shows the TGA-H_2 obtained with the support and the catalysts. The curves are broad, and the onset of reduction follows the weight loading in the order 8V < 3.5V < 1V, with reduction for each sample completed by ~873 K. This difference in onset of reduction may be attributed to different reducibility of vanadia species, monovanadates, polyvanadates, and V_2O_5 coexisting on the catalysts' surfaces. The weight loss at the reduction step increased with vanadia loading: 0.3% for 1V, 1.1 for 3.5V, and 2.1% for 8V. Translating these weights into oxygen loss reveals a 1:1 relationship between vanadium atoms and oxygen atom loss (Table 2). This suggests a 2-point change in the vanadium oxidation state; therefore, if the vanadium was in a 5+ oxidation state before reduction, then it would convert to 3+ after reduction. This was investigated by in situ UV–visible DRS (Fig. 3). Before reduction, the catalysts were in a V^{5+} oxidation state with typical charge transfer bands at 267 nm (37,450 cm^{-1}) for 1V, 290 nm (34,480 cm^{-1}) for 3.5V, and 357 nm (28,000 cm^{-1}) for 8V. This change in position of the charge transfer band is indicative of the increasing polymeric nature of the vanadia [25]. Over the course of the reduction, the spectrum changed (Fig. 4) to give a spectra typical for a V^{3+} state with d–d transitions at around 575 nm (17,390 cm^{-1}) for 3.5V and 625 nm (16,000 cm^{-1}) for 8V. However the 1V spectrum is more indicative of V^{4+}, with a single band at 585 nm (17,090 cm^{-1}).

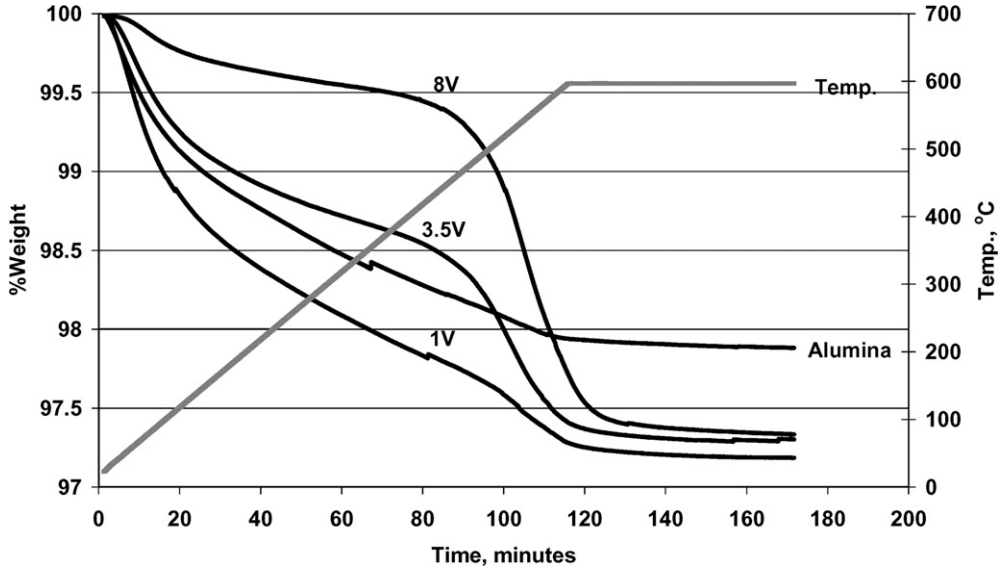

Fig. 2. TGA-H_2 of the support and catalysts.

Table 2
TGA-H_2/Ar of the catalysts

Catalyst	V atoms in 1 g	O atoms removed from 1 g	V:O ratio
1V	1.18×10^{20}	1.13×10^{20}	1.0:1
3.5V	4.13×10^{20}	4.14×10^{20}	1.0:1
8V	9.45×10^{20}	7.90×10^{20}	1.2:1

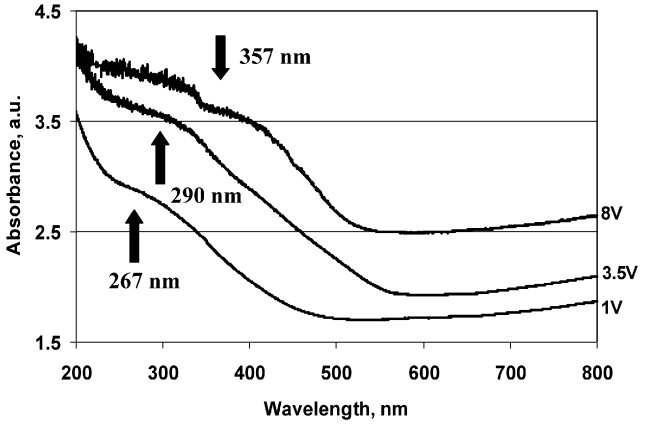

Fig. 3. UV–visible spectra of the fresh catalysts.

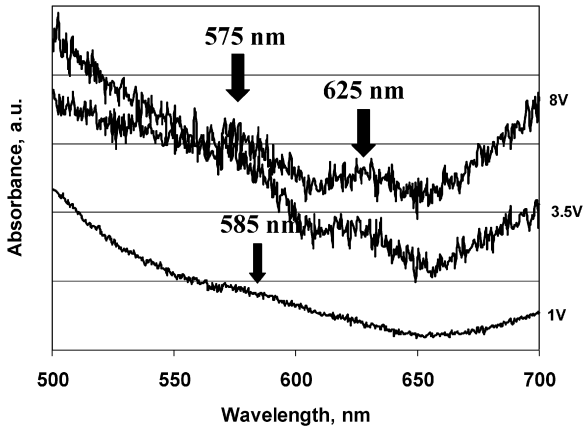

Fig. 4. UV–visible spectra of the reduced catalysts.

Given that active vanadium surface species and their reduction behaviours are important parameters that may determine the alkane dehydrogenation activity [25–27], further investigation of the reduced species was undertaken using dioxygen chemisorption at 293 and 873 K. Bulk reoxidation at 873 K can be directly compared with the TGA-H_2 weight loss figures. In earlier work [23], we had used the bulk uptake figures as a measure of an average vanadium oxidation state when the catalyst was reduced. By this method, the average oxidation state of the 1% VO_x/alumina was calculated as 3.8, whereas the average oxidation state for the 3.5% VO_x/alumina was calculated as 2.6. Both of these figures are in excellent agreement with the findings from UV–visible DRS. The bulk reoxidation data in conjunction with the TGA results indicate that for the 1V catalyst containing principally isolated vanadate species, only 66% of the oxygen removed can be replaced. For the 3.5V catalyst, all of the oxygen removed can be replaced, whereas for the 8V catalyst, 141% of the oxygen removed can be replaced.

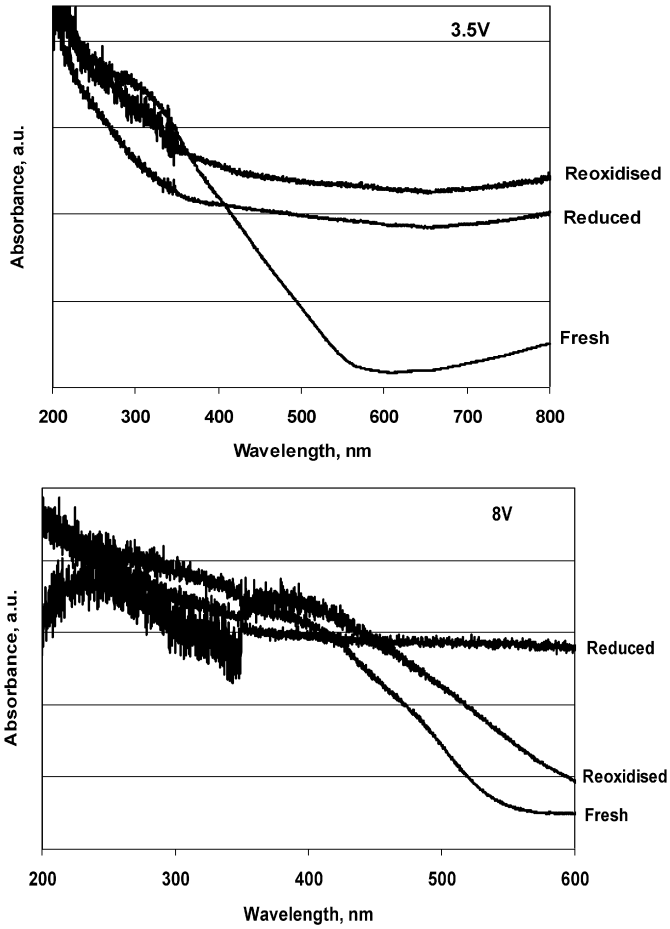

Fig. 5. UV–visible DRS spectra—reduction and reoxidation.

This trend in difficulty of oxygen replacement also has been observed in TEOM studies [28] and is also seen in the UV–visible DRS. Once reduced, the 3.5V sample did not regain its original state even after high-temperature oxidation; however, the reduced 8V sample did convert to a species similar to the original state (Fig. 5).

3.1. Dehydrogenation of n-butane

Various aspects of supported vanadia catalysts have been extensively studied for both the direct and oxidative dehydrogenation of *n*-butane [8,29–32]. Dehydrogenation of *n*-butane was studied for the catalysts as well as for the support θ-alumina. Fig. 6 shows activity profiles for the fresh and regenerated catalysts. The conversions and product distributions (analysis at 15 min) of fresh and regenerated catalysts are given in Tables 3 and 4, respectively. The alumina support yielded only cracked products, with the yield of C1–C3s remaining the same after vanadia incorporation, indicating that the alumina was the principal source of the cracked products formed over the catalysts. Previous characterisation by Raman spectroscopy [22] revealed that isolated VO_x species dominated at surface densities <1 V/nm^2; polyvanadates coexist with monovanadates at surface densities of 1.2–4.4 V/nm^2; and V_2O_5 formed at surface density >4.4 V/nm^2. Therefore, it is worthwhile to

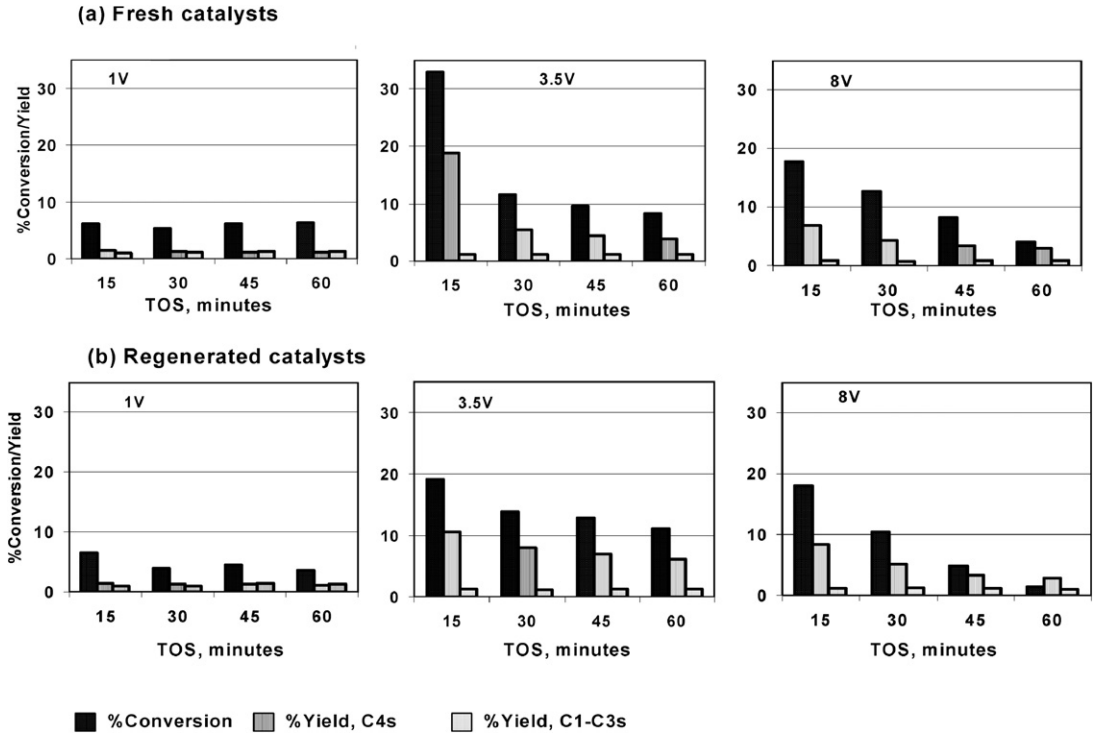

Fig. 6. *n*-Butane dehydrogenation: %conversion and yield of products.

Table 3
Dehydrogenation of *n*-butane—%conversion and product distribution. (Fresh catalysts—analysis at 15 min)

Sample	%Conv.	%Selectivity (yield)				
		1-Butene	Trans-2-butene	Cis-2-butene	1,3-Butadiene	C1–C3s
θ-Alumina	5.8	0.73 (0.04)	0.60 (0.03)	–	–	21.2 (1.2)
1V	6.3	9.03 (0.6)	7.81 (0.5)	6.1 (0.4)	–	16.9 (1.07)
3.5V	32.9	20.4 (6.7)	16.9 (5.6)	13.1 (4.3)	5.7 (1.9)	3.4 (1.1)
8V	17.8	15.9 (2.8)	12.7 (2.3)	9.9 (1.7)	–	5.1 (0.9)

Table 4
Dehydrogenation of *n*-butane—%conversion and product distribution. (Regenerated catalysts—analysis at 15 min)

Sample	%Conv.	%Selectivity (yield)				
		1-Butene	Trans-2-butene	Cis-2-butene	1,3-Butadiene	C1–C3s
θ-Alumina	5.8	1.12 (0.07)	0.8 (0.05)	–	–	32.7 (1.9)
1V	6.6	9.1 (0.6)	7.7 (0.5)	5.9 (0.4)	–	15.9 (1.1)
3.5V	19.1	20.6 (3.9)	16.7 (3.2)	13.0 (2.5)	4.1 (0.8)	6.5 (1.2)
8V	18.0	19.2 (3.5)	15.5 (2.8)	12.1 (2.2)	–	6.6 (1.2)

Table 5
Rate of reaction and turn over frequencies with time on stream

TOS (min)	Rate (μmol g^{-1} s^{-1})			TOF (s^{-1})		
	1V	3.5V	8V	1V	3.5V	8V
15	1.1	20.3	5.8	0.051	0.269	0.037
30	1.0	5.8	3.7	0.047	0.077	0.023
45	1.0	4.7	2.9	0.044	0.063	0.018
60	1.0	4.2	2.5	0.044	0.056	0.016
75		4.2	2.2		0.056	0.014
105	0.9	3.5		0.041	0.046	

examine the rate and TOF as functions of vanadium loading (Table 5). TOFs were calculated using the oxygen adsorption data at 293 K as measures of surface site density. Both the rate and TOF data that the sample with the highest proportion of polvanadate species (3.5V) is the most effective dehydrogenation catalyst. These results are in keeping with earlier studies on ODH of propane using vanadia catalysts, where the data indicated that the monovanadate structure was significantly less active than polyvanadates [24]. The V–O–Al species present in monovanadate structures appear to be more difficult to re-

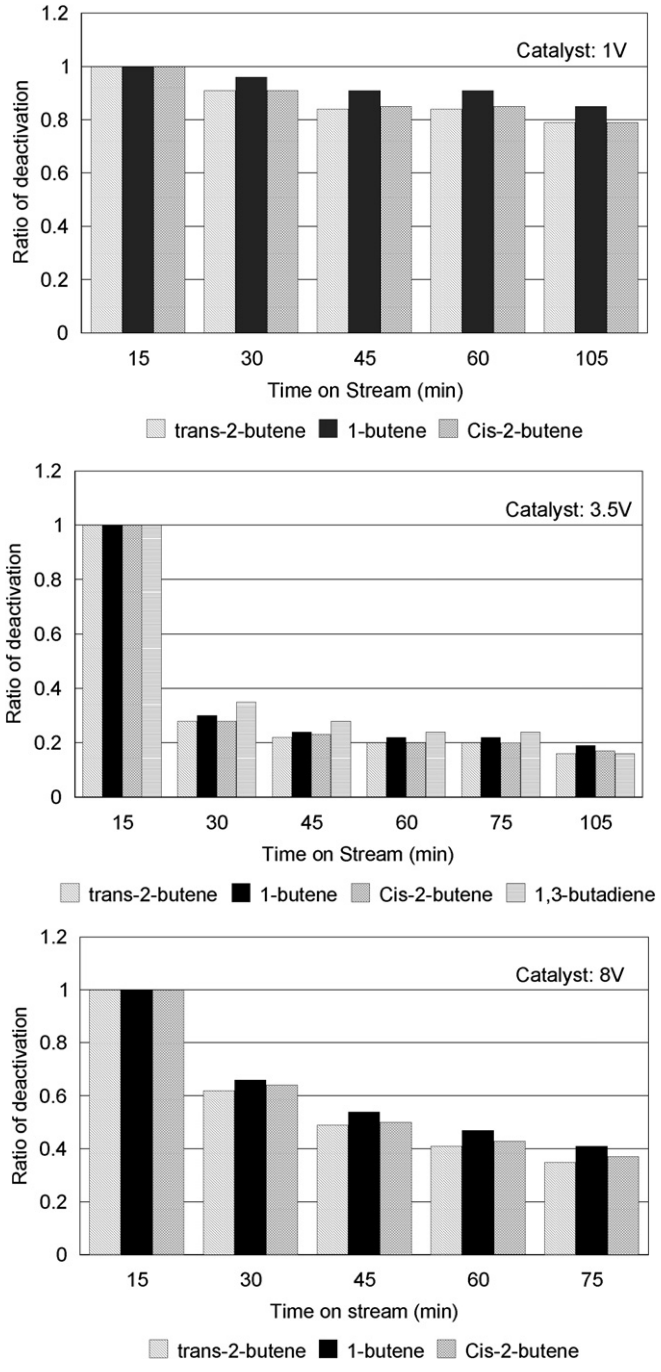

Fig. 7. Ratio of deactivation for butene isomers.

duce than V–O–V or V=O sites in polyvanadates, consistent with the findings of reducibility studies in this study and earlier studies [22].

The dependence of conversion/yield on time on stream is different for catalysts with different surface vanadia species. The 3.5V catalyst, which contains mainly polyvanadate surface species, gave the highest initial conversion but also exhibited the most significant deactivation. After regeneration, however, the 3.5V catalyst became more stable to deactivation, possibly reflecting the change in surface species as identified by UV–visible DRS. In comparison, the 1 and 8V catalysts showed no significant difference in behaviour after regeneration. 1,3-Butadiene appeared as one of the reaction products only when 3.5V was used for dehydrogenation, emphasizing the high activity and selectivity of polyvanadate species toward dehydrogenation.

Table 6
Product composition (%) of butenes and 1,3-butadiene

Catalyst	C-4 product composition (%)			
	Trans-2-butene	1-Butene	Cis-2-butene	1,3-Butadiene
Equilibrium	34.2	27.1	34.1	4.6
1V, 15 min	34.0	39.4	26.5	0.0
30 min	32.8	41.3	25.9	0.0
3.5V, 15 min	30.2	36.3	23.3	10.2
30 min	28.3	37.8	22.3	11.5
8V, 15 min	33.0	41.2	25.7	0.0
30 min	31.0	43.9	25.1	0.0

Comparison of deactivation on a product basis revealed that the rate of deactivation was not identical for the butane isomers (Fig. 7). The rate of decay of 1-butene was systematically lower over each of the catalysts. Considering the ratio of butenes produced during the course of the reaction over the three catalysts provides more insight into the reaction sequence (Table 6). Although 1-butene was the least thermodynamically favoured isomer, it was always present above the equilibrium value and became more dominant as the catalyst deactivated. Similarly, the equilibrium ratio of trans:cis was ∼1:1, yet the ratio typically was >1.25:1. Achieving this behaviour requires various processes. First, any butane isomerisation must be slow, and the deactivation of the isomerisation site must be faster than that of the dehydrogenation site. Second, the primary product must be 1-butene, which then isomerises to trans-2-butene. Note that 1-butene cannot isomerise to solely to cis-2-butene, but can possibly isomerise to both 2-butene isomers, with a bias toward the trans isomer.

Carbon deposition is the main cause of deactivation in alkane dehydrogenation catalysts. Deposition of carbon occurs through progressive dehydrogenation, condensation, polymerisation, and cyclisation of hydrocarbon species on the catalyst surface. Olefinic precursors formed on the metal active sites are known to migrate to the support and convert through condensation and polymerisation reactions to form polyolefinic/polyaromatic/graphitic types of coke [33–35]. Temperature-programmed techniques have been used to study gasification of coke on spent catalyst surfaces [36]. In the present study, we used TPO and microanalysis (of C and H) of spent catalysts to probe catalyst deactivation.

As expected, online MS indicated that all hydrocarbon components were rapidly swept out of the reactor at 873 K when the gas stream was switched from butane to argon, and no other gases apart from the argon carrier were detected during the cool-down period. However, when 2% O_2/Ar was passed over the sample at room temperature, C4 species were evolved. Fig. 8 shows the evolution of butane, butanes, and butadiene from the three catalysts and the alumina support. From the desorption profiles, it can be seen that the amount of retained C4 was proportional to the amount of VO_x on the surface. These species were desorbed from the catalyst on contact with oxy-

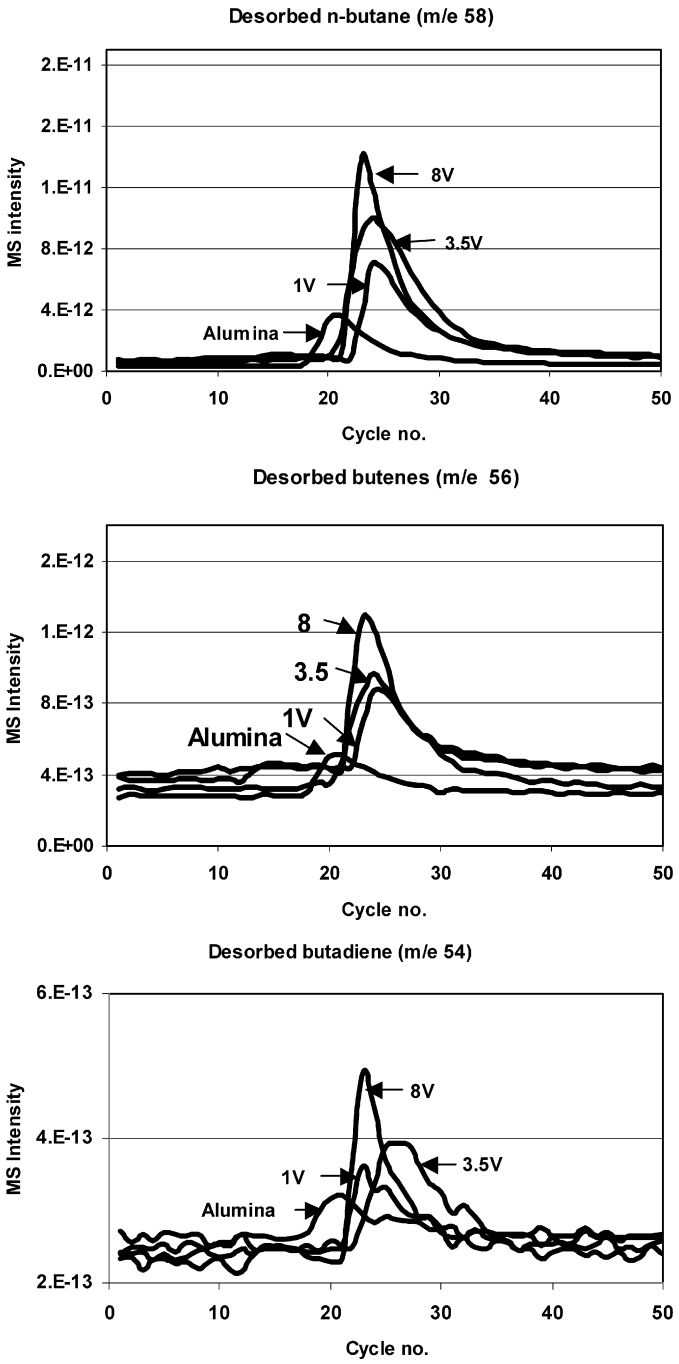

Fig. 8. Desorption of butane, butenes and butadiene at room temperature. Masses used for analysis were 58 for butane, 41 for butene, and 39 for butadiene as these are m/es, which are not affected by the other products to any great extent.

gen at room temperature. The finding of desorption of C4 gases, which are strongly adsorbed and stable at 873 K in an inert atmosphere but are easily displaced by an oxidising gas at room temperature, is surprising. This desorption process can be viewed as an oxidative displacement, resulting in recombination of reaction intermediates (hydrogen and alkyl, alkenyl, and alkadienyl) from the surface of reduced VO_x species and acid sites on the alumina. To understand the effect of these species on deactivation, the gas flow was switched back to argon and the catalyst was reheated to 873 K, at which point the flow was switched to butane and the activity was measured. The activity recorded was >75% of that regained after a full regeneration involving heating in O_2/Ar at 873 K (Fig. 9). Indeed, after 1 h on stream, there was no detectable difference between room temperature regeneration and regeneration at 873 K. When a TPO was run following this desorption, combustion of carbon was observed. This reaction/regeneration cycle was repeated, and similar evolution of C4 gases at room temperature was observed (not shown). The TPO patterns of first use and regenerated catalysts, shown in Figs. 10 and 11, demonstrate the presence of different types of coke species on the catalyst surfaces over and above the C4 gases that are desorbed at room temperature. Note that the removal of this coke had little effect on the regeneration of activity, suggesting that much of the polyaromatic/polyolefinic/graphitic coke identified by spectroscopy was associated not with the VO_x species, but rather with the support. The TPO of the 3.5V fresh catalyst after reaction indicated two different types of coke species, whereas that of regenerated catalyst showed only one peak. The temperature profile was not linear over the complete range, which could potentially lead to artefacts; however, the TPOs of the fresh and regenerated catalysts exhibited identical temperature profiles and thus should have been internally consistent. These results are in agreement with the reactivity profile and the UV–visible DRS in recording a change between the fresh and regenerated catalysts.

Spent catalysts after *n*-butane dehydrogenation activity evaluation were analysed for total C and H content; the results are reported in Table 7. The amount of carbon on the used support could not be measured by the elemental analyser even though the support appeared light black in colour. The C:H ratio of 1V catalyst after evaluation was found to be 0.9, very close to that of polystyrene monomer [23]. However, the C:H ratio for the 3.5V spent catalyst was much higher than that for both the 1 and 8V catalysts, suggesting the presence of highly carbonaceous polyaromatic or graphitic carbon on the surface. The variation in the C:H ratio was as would be expected from the TPO data, with each catalyst having differing species present. The amount of carbon found on each catalyst also was in agreement with the TPO findings, exhibiting an order of carbon deposition of alumina of < 1V < 3.5V < 8V. Note that these analyses required exposure of the catalyst to air at room temperature, causing the catalyst to lose adsorbed butane, butanes, and butadiene. The findings indicate that the VO_x species plays a role in the generation of the non-C4 carbonaceous deposit, suggesting either that spillover occurs from the VO_x to the support or that there are VO_x sites that catalyse production of coke but do not catalyse dehydrogenation.

4. Conclusions

Our UV–vis spectroscopic characterisation and oxygen chemisorption study of 1, 3.5, and 8% VO_x/θ-alumina catalysts combined with testing and TPO have revealed much about the nature of the active species and the cause of catalyst deactivation. The catalyst with a 1% V loading (1V) exhibited

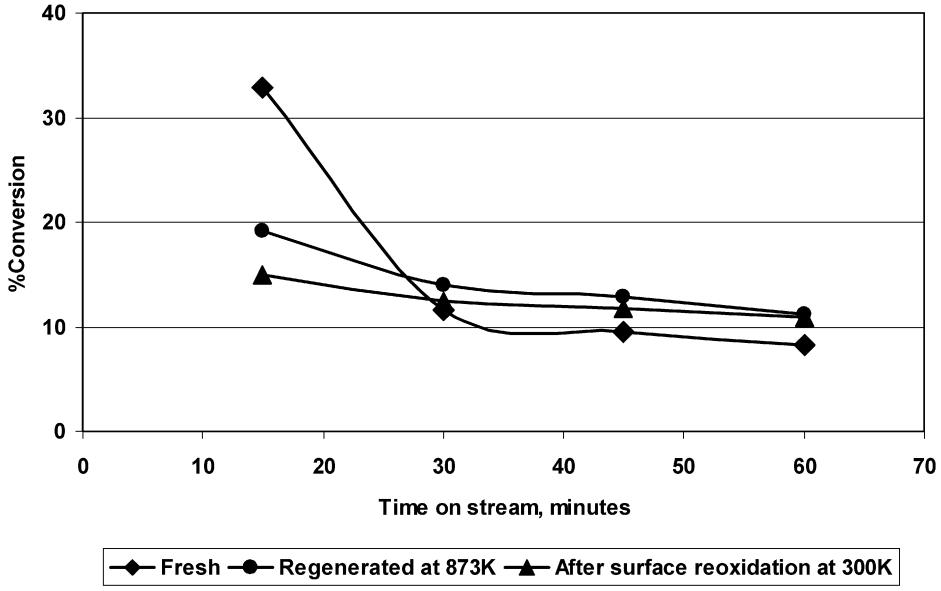

Fig. 9. Regained dehydrogenation activity after surface and bulk reoxidation.

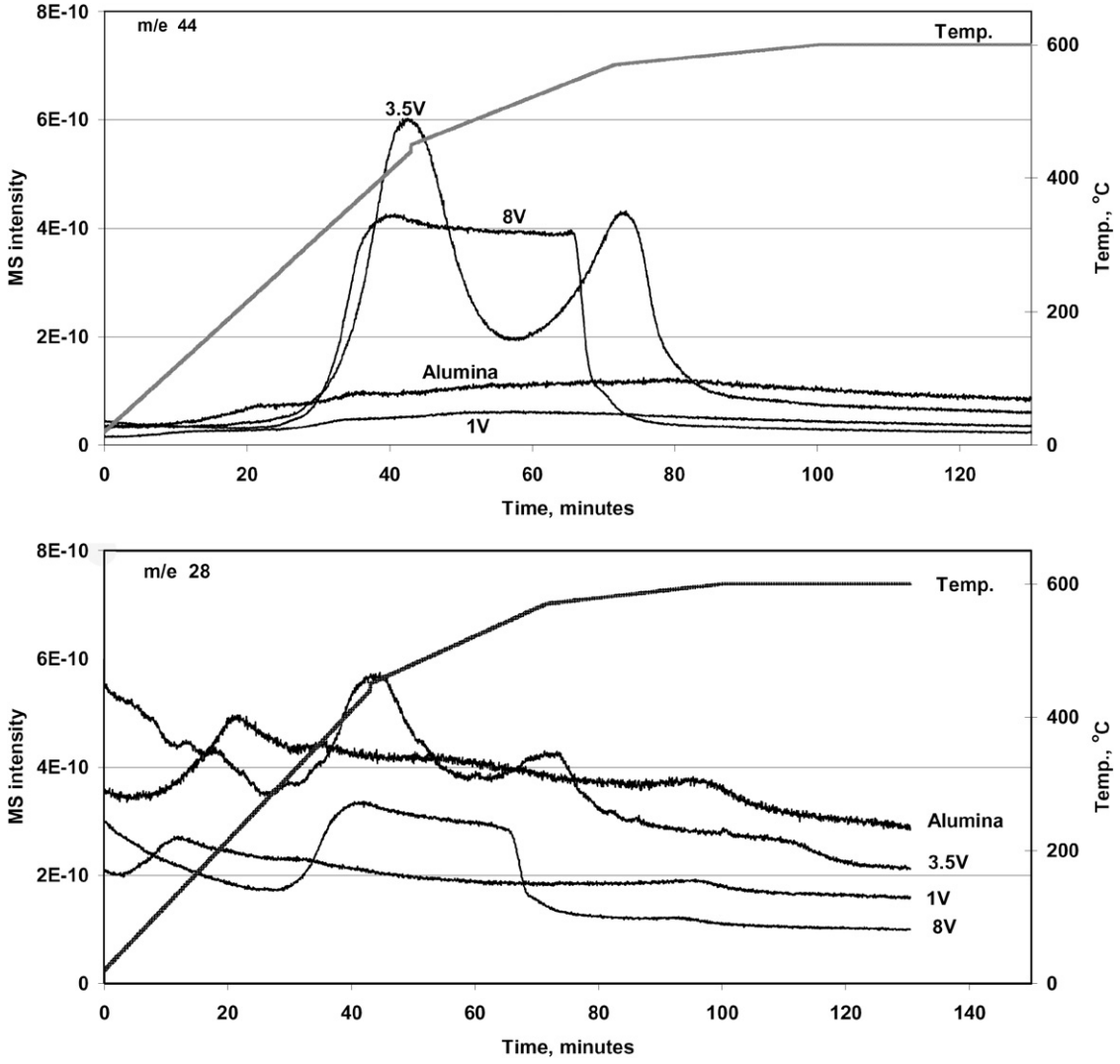

Fig. 10. TPOs of catalysts after *n*-butane dehydrogenation.

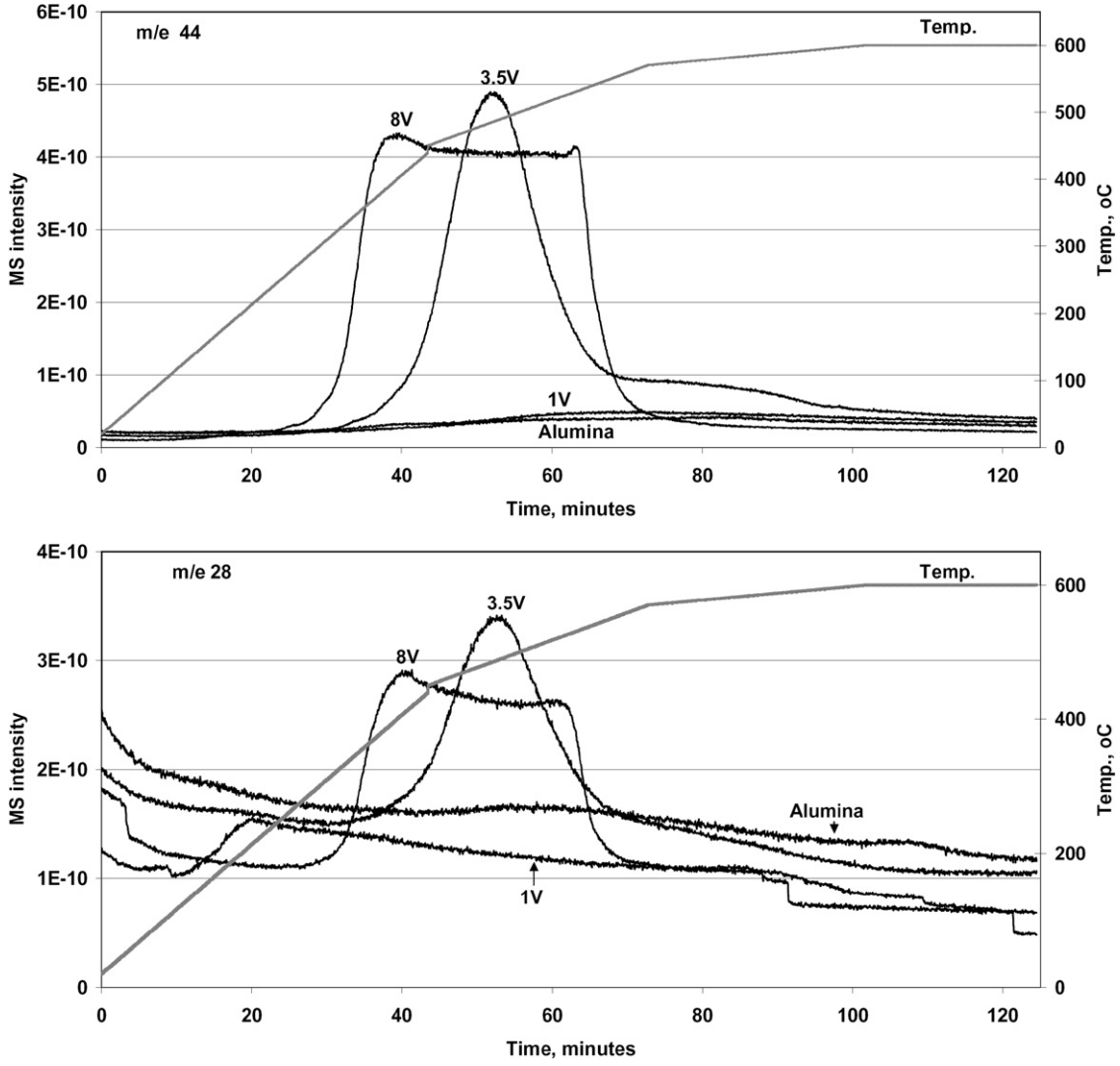

Fig. 11. TPOs of regenerated catalyst after second *n*-butane dehydrogenation period.

Table 7
Microanalysis data of spent catalysts

Spent catalyst	%C	%H	C:H
θ-Alumina	N.D.[a]	0.36	–
1 A	2.3	0.2	0.9
3.5 V	4.2	0.1	3.5
8V	4.9	0.25	1.6

[a] Not detected.

a 4+ oxidation state after reduction and existed principally as a monovanadate [22]. This species gave a low TOF for butane dehydrogenation and a high selectivity for carbon laydown. In contrast, the 3.5% V-loaded catalyst (3.5V) reduced to give a 3+ oxidation state and the highest proportion of polyvanadate species [22]. This catalyst had the highest TOF for butane dehydrogenation and was the most effective catalyst. The 8% V loaded catalyst (8V) contained significantly more V_2O_5 than 3.5V but also reduced to a 3+ oxidation state; however, it was noticeably less effective at butane dehydrogenation. Taken together, these results and those from the literature reveal that the optimum species for dehydrogenation is a reduced polyvanadate. The exact nature of the species (e.g., the optimum polyvanadate array size), requires further investigation.

We found that the primary product of butane dehydrogenation was 1-butene, which then isomerised to trans-2-butene. Rather surprisingly, butane isomerisation was slow, and the deactivation profiles of the butanes showed sites that catalysed dehydrogenation and sites that catalysed butane isomerisation. The isomerisation site deactivated faster than the dehydrogenation site, leading to an enhanced selectivity to 1-butene with increasing time on stream.

It has long been assumed that deactivation in these systems is due to carbon laydown and the formation of polynuclear aromatics. However, in this study we have been able to show that >75% of the observed catalyst deactivation is due not to polynuclear aromatics, but rather to strongly bound reaction intermediates. These intermediates can be removed from the surface under mild conditions, as butane, butanes, and butadiene, by treatment in 2% O_2/Ar at room temperature. This discovery has implications for catalyst regeneration and maintenance of activity.

This is not to say that polynuclear aromatics are not formed. Indeed, TPO and Raman analysis [23] has revealed that polynuclear aromatics are formed and have differing natures depending on the vanadia species. However, they have little influence on catalyst deactivation in the early stages. Clearly, pore blocking by these large entities can be expected to influence the reaction over time. The amount of carbon retained by each catalyst after removal of the reaction intermediates was alumina $< 1V < 3.5V < 8V$, indicating that VO_x species also played a role in the generation of the non-C4 carbonaceous deposit. Our findings also indicate that spillover from the VO_x to the support occurred and that some VO_x sites catalysed coke production. The possibility of producing polyvanadates that catalyse dehydrogenation but not carbon laydown is a tantalising prospect. Minor C1–C3 products were formed over the alumina support and were generally independent of vanadia loading, suggesting that they had little effect on formation of the polynuclear aromatics.

This new understanding of the mechanism of catalyst deactivation has significant implications for catalyst and process design. Currently aggressive combustion of retained carbon, in all its forms, is used not only to regenerate the catalyst, but also to balance the heat requirements. It is possible to envision a future catalyst in which no polynuclear aromatics are deposited and any regeneration is subtly done in situ with little heat generation, presenting new challenges to the process engineer.

Acknowledgments

Support was provided by the Engineering and Physical Sciences Research Council and Johnson Matthey plc under the ATHENA grant. The authors thank Professor Peter Stair, Dr. Zili Wu, Professor Lynn Gladden, and Dr. James McGregor for very helpful discussions.

References

[1] T. Hutson Jr., W.C. McCarthy, in: R.A. Meyersn (Ed.), Handbook of Petroleum Refining Processes, McGraw–Hill, London, 1986.
[2] P.R. Pujado, B.V. Vora, Hydrocarbon Process. 65 (1990).
[3] G.F. Hornaday, F.M. Ferrell, G.A. Mills, Adv. Petrol. Chem. Refining 4 (1961) 451.
[4] J.R. Butt, in: J.R. Anderson, M. Boudart (Eds.), Catalysis, Science and Technology, vol. 6, Springer, Berlin, 1984, p. 16.
[5] G.C. Bond, Appl. Catal. A Gen. 149 (1997) 3.
[6] J.M. McNamara, S.D. Jackson, D. Lennon, Catal. Today 81 (2003) 583.
[7] S.D. Jackson, P. Leeming, J. Grenfell, J. Catal. 150 (1994) 170.
[8] I.E. Wachs, B.M. Weckhuysen, Appl. Catal. A Gen. 157 (1997) 67.
[9] J.N.J. van Lingen, O.L.J. Gijzeman, B.M. Weckhuysen, J.H. van Lenthe, J. Catal. 239 (2006) 34.
[10] M.L. Ferreira, M. Volpe, J. Mol. Catal. A Chem. 164 (2000) 281.
[11] X. Gao, I.E. Wachs, J. Catal. 192 (2000) 18.
[12] J.M. Kanervo, M.E. Harlin, A.O.I. Krause, M.A. Bañares, Catal. Today 78 (2003) 171.
[13] O.L.J. Gijzeman, J.N.J. van Lingen, J.H. van Lenthe, S.J. Tinnemans, D.E. Keller, B.M. Weckhuysen, Chem. Phys. Lett. 397 (2004) 277.
[14] H.J. Freund, Catal. Today 100 (2005) 3.
[15] E.M. Garcia, M.D. Sanchez, G. Tonetto, M.A. Volpe, J. Colloid Interface Sci. 292 (2005) 179.
[16] B. Olthof, A. Khodakov, A.T. Bell, E. Iglesia, J. Phys. Chem. B 104 (2000) 1516.
[17] J.M. Jehng, G. Deo, B.M. Weckhuysen, I.E. Wachs, J. Mol. Catal. A 110 (1996) 41.
[18] G.T. Went, S.T. Oyama, A.T. Bell, J. Phys. Chem. 94 (1990) 4240.
[19] M.M. Koranne, J.G. Goodwin, G. Marcelin, J. Catal. 148 (1994) 369.
[20] M.E. Harlin, V.M. Niemi, A.O.I. Krause, B.M. Weckhuysen, J. Catal. 203 (2001) 242.
[21] U. Bentrup, A. Martin, G.U. Wolf, Thermochim. Acta 398 (2003) 131.
[22] Z. Wu, H.S. Kim, P.C. Stair, S. Rugmini, S.D. Jackson, J. Phys. Chem. B 109 (2005) 2793.
[23] S.D. Jackson, S. Rugmini, P.C. Stair, Z. Wu, Chem. Eng. J. 120 (2006) 127.
[24] A. Khodakov, B. Olthof, A.T. Bell, E. Iglesia, J. Catal. 181 (1999) 205.
[25] F. Arena, F. Frusteri, G. Martra, S. Coluccia, A. Parmaliana, J. Chem. Soc. Faraday Trans. 93 (1997) 3849.
[26] M. Faraldos, J.A. Anderson, M.A. Bañares, J.L.G. Fierro, S.W. Weller, J. Catal. 168 (1997) 110.
[27] M. Faraldos, M.A. Bañares, J.A. Anderson, H. Hu, I.E. Wachs, J.L.G. Fierro, J. Catal. 160 (1996) 214.
[28] J. McGregor, L. Gladden, unpublished work.
[29] B.M. Weckhuysen, D.E. Keller, Catal. Today 78 (2003) 25.
[30] A. Klisinska, A. Haras, K. Samson, M. Witko, B. Grzybowska, J. Mol. Catal. A Chem. 210 (2004) 87.
[31] A.A. Lemonidou, Appl. Catal. A Gen. 216 (2001) 277.
[32] J.M. Lopez Nieto, P. Concepcion, A. Dejoz, H. Knozinger, F. Melo, M.I. Vazquez, J. Catal. 189 (2000) 147.
[33] J.R. Rostrup-Nielsen, in: J.R. Anderson, M. Boudart (Eds.), Catalysis, Science and Technology, vol. 5, Springer, Berlin, 1984, chap. 1.
[34] J.R. Rostrup-Nielsen, P.E. Hojlund Nielsen, in: J. Oudar, H. Wise (Eds.), Deactivation and Poisoning of Catalysts, Dekker, New York, 1985, chap. 7.
[35] S.K. Sahoo, P.V.C. Rao, D. Rajeshwer, K.R. Krishnamurthy, I.D. Singh, Appl. Catal. A Gen. 244 (2003) 311.
[36] C.A. Querini, S.C. Fung, Catal. Today 37 (1997) 277.